ELSEVIER

Earth and Planetary Science Letters 206 (2003) 173–186

EPSL

www.elsevier.com/locate/epsl

Particle size distributions in natural carbonate fault rocks: insights for non-self-similar cataclasis

Fabrizio Storti *, Andrea Billi, Francesco Salvini

Dipartimento di Scienze Geologiche, Università degli Studi 'Roma Tre', Largo S.L. Murialdo 1, I-00146 Rome, Italy

Received 18 July 2002; received in revised form 8 November 2002; accepted 8 November 2002

Abstract

Particle size distributions of cataclastic rocks influence the mechanical and fluid flow behaviour of fault zones. Available data from natural cataclastic rocks are still controversial and do not fully support a self-similar evolution for the cataclastic process, a concept derived from laboratory experiments and micromechanical modelling. Our analyses of particle size in carbonate fault rocks show power law distributions with fractal dimensions spanning a broad range. This confirms that the idea of a persistent fragmentation mechanism for describing the entire evolution of natural cataclastic fault cores in carbonate rocks is inadequate. Conversely, we propose that the fragmentation mechanism progressively changes with the intensity of comminution. Slip localisation within narrow shear bands is favoured when a favourable cataclastic fabric with fractal dimensions $D \sim 2.6$–2.7 is achieved in the fault zone. Intense comminution in the narrow shear zones produces the preferential formation of small diameter particles resulting in particle size distributions characterised by D values approaching or exceeding 3. The non-self-similar evolution of natural cataclastic rocks has an important impact on the frictional and permeability properties of fault zones.

Keywords: fault rocks; cataclasis; particle size; fractal; permeability

1. Introduction

Cataclasis is the process of progressive fragmentation, grinding and compaction of rock particles [1]. During faulting, cataclasis can eventually produce fault gouges, i.e. fault rocks that have been ground to a very fine-grained powder or clayey material retaining few larger survivor grains [2]. Cataclastic rocks, and in particular fault gouges, control the frictional fault properties [3–6] and the three-dimensional permeability patterns around faults [7,8]. For this reason, they have been extensively studied in the field [9–21], in laboratory experiments [3,4,9,11,22–31] and by analytical modelling [13,32–34]. Numerical modelling has also been used to examine the influence of particle size distribution and inter-particle friction on the nature of deformation in granular fault gouges and on their mechanical behaviour [35].

Many solutions have been proposed for de-

* Corresponding author. Tel.: +39-6-54888085; Fax: +39-6-54888201.
E-mail address: storti@uniroma3.it (F. Storti).

0012-821X/02/$ – see front matter
PII: S0012-821X(02)01077-4

scribing cataclastic rock particle size distribution in both two and three dimensions. They include both incremental and cumulative relations between mass/volume/number and increasing or decreasing mass/size [14]. It has been demonstrated that the best way to characterise particle size distributions [13,14] is by using the fractal relationship of particle frequency by size:

$$N(S) \approx S^{-D} \quad (1)$$

where $N(S)$ is the number of particles less than size S and D is the fractal dimension. The coefficient D is conveniently determined as the slope of the best fit line on a log $N(S)$ against log S graph.

Different values of D are expected for different fragmentation processes. In particular, three theories of fragmentation have been directly expressed in three-dimensional fractal terms [14]: (i) the 'pillar of strength' model of [32], which predicts a D value equal to 1.97; (ii) the 'plane of fragility' model of [33], which predicts a D value equal to 2.84; (iii) the 'constrained comminution' model of [13], which predicts a D value equal to 2.58. Experimental work on simulated fault gouges has shown their tendency to develop D values of about 2.6 [24,26,27], supporting the 'constrained comminution' model of [13]. In particular, [27] showed that $D \approx 2.6$ may represent a steady-state value reached after an initial amount of displacement from early values of about 1.8. Only D values in experimental shear bands approached 3 [26] or 4 [27].

Fractal dimensions measured in natural cataclastic rocks are more controversial. Results from faults in crystalline basement rocks gave either D values averaging 2.6 [13,36] or a great variability in fractal dimensions, ranging from 1.88 to 5.52 [9,14,19]. Such large variability of D values is unexpected in a self-similar cataclastic process [24], where the progressive breakdown of particles is controlled by a scale- and time-independent fragmentation mechanism. In particular, the 'constrained comminution' model of [13], which is based on the assumption that the failure probability of particles depends largely on the relative size of nearest neighbours, predicts the tendency for cataclastic rocks to develop a self-similar grain size distribution having a constant fractal dimension equal to 2.58. This D value ($D = 2.58$), in fact, describes a cataclastic fabric that minimises the fracture probability of particles having similar dimensions [13].

Preferential fragmentation of large particles is a possible explanation for the occurrence in cataclastic rocks of D values significantly higher

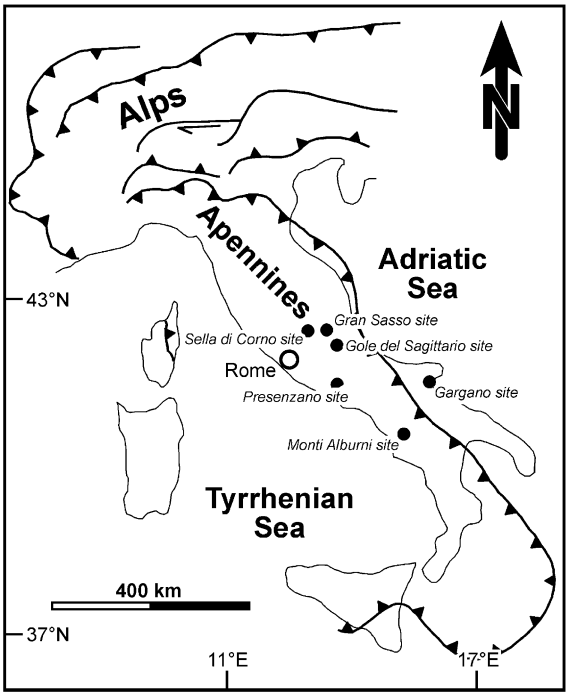

Field site	Label	Latitude	Longitude
Gargano	GA, MA	41°43'10"N	13°36'16"E
Gole del Sagittario	SA	41°58'04"N	13°48'32"E
Gran Sasso	GS, RIO, SC, CI	42°21'03"N	13°36'16"E
Monti Alburni	AL	41°31'03"N	15°27'44"E
Presenzano	PR	41°26'01"N	14°02'58"E

a)

Field site	$\%CaCo_3$	$\%MgCo_3$	% insoluble residual
GA	95.6	2.7	1.7
SA	97.6	2.1	0.3
SC	96.6	2.4	1.0
AL	96.1	3.1	0.8
PR	98.2	1.9	0.1

b)

Fig. 1. (a) Location map of the sampled fault zones. (b) Chemical analysis of the protolith rocks in the studied fault sites.

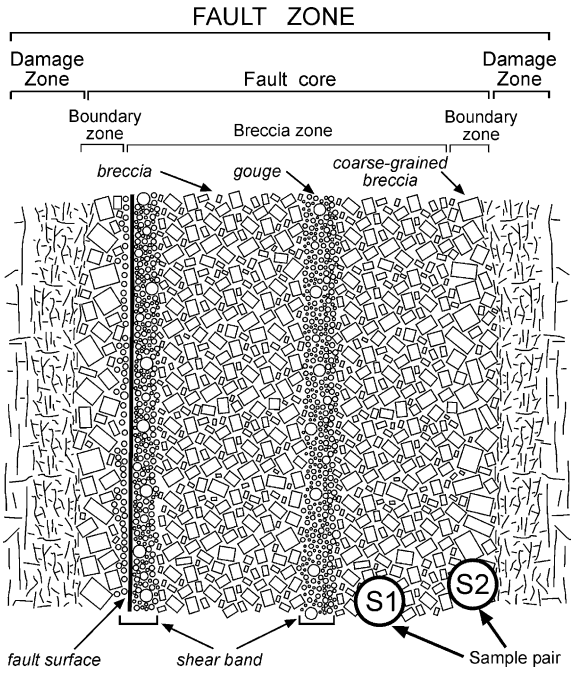

Fig. 2. Conceptual sketch of a fault zone sectioned perpendicular to the shear direction. The main sectors, characterised by different fabrics and particle size distributions, are schematically highlighted. Not to scale.

than 2.58. This mechanism has been proposed for experimental shear bands by [27] and for natural cataclastic rocks by [14], who also pointed out the importance of factors such as rock type, alteration, and fault kinematics on the final particle size distribution. An additional mechanism for explaining the development of fractal dimensions significantly higher than 2.58 is the preferential increase of small particles by rotation-enhanced abrasion of larger particles during shear [19,37]. The first mechanism is mainly related to the state of stress within the deforming cataclastic rocks, while particle grinding essentially depends on slip-enhanced rolling and shearing. Both mechanisms likely determine the evolution of particle size distributions in shear bands. Their relative contribution is expected to vary through time.

The objective of our study is to get further insights into the progression of cataclasis during faulting. We studied particle size distributions of cataclastic rocks developed along outcrop-scale strike-slip and extensional faults affecting platform carbonate in the Apennines, Italy. Protolith rocks in all studied field sites are mostly composed of $CaCO_3$ and are characterised by very small amounts of insoluble materials (Fig. 1). The structural architecture of the fault zones (Fig. 2) is composed of heavily fractured damage zones which bound the fault core where most of the displacement is accommodated [8,16]. The fault cores have a cross-sectional width varying from about 0.3 m to 2.6 m. We sampled boundary zones adjacent to the damage zone (Fig. 3a), breccia zones constituting the bulk of fault core rocks (Fig. 3b), and shear bands within fault cores (Fig. 3c). Sampled cataclastic rocks are mainly non-cohesive to poorly cohesive breccias in the boundary zones and breccia zones, and gouges in the shear bands.

Particle sizes are power-law-distributed over the analysed size range and their fractal dimensions have a large variability. In the following, we discuss the relations between D values and the structural architecture of fault cores as well as the implications for the evolution of the cataclastic process.

2. Particle size analysis

2.1. Methodology

Sampled cataclastic rocks (49 samples) were analysed using a sieving and weighing technique [24]. Samples were fully disaggregated by a non-destructive ultrasonic device, dried for 24 h at 110°C, and sieved in a standard dry sieve array (Table 1 in the **Background Data Set**[1]). Inspection of the sieved material allowed removal of grains in case they were made up of still cemented cataclasite. This prevented the possible coarseward bias of the particle size populations. The dry weight of residual material in each sieve was transformed to the equivalent particle number by assuming that the grain shapes can be approximated by spheres [37]. The total weight in each sieve was divided by the weight of the sphere with

[1] http://www.elsevier.com/locate/epsl

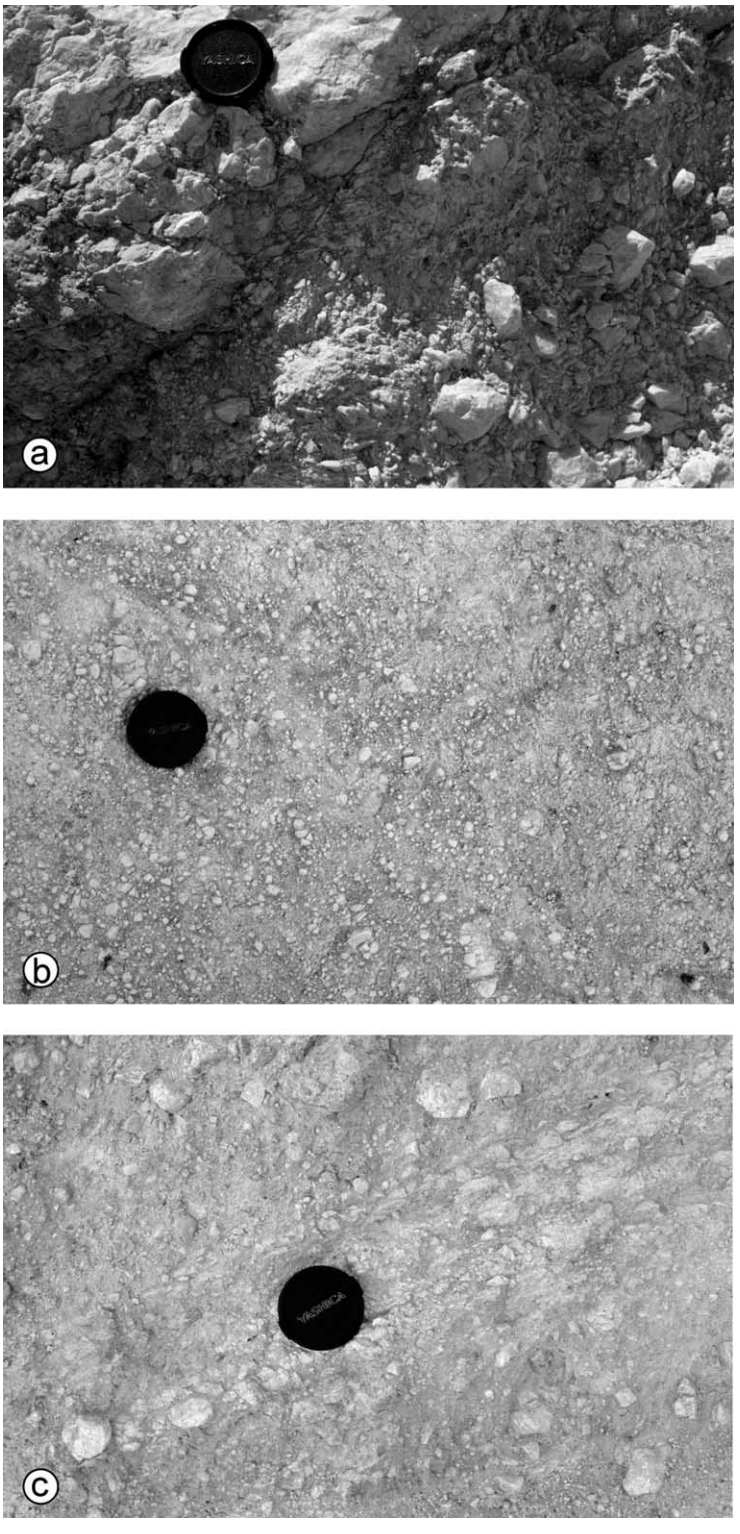
a
b
c

the same diameter as the mesh aperture of the overlying sieve. A density of 2670 kg/m^3 was used for computing the weight of the reference spheres. The use of different reference values such as the weight of the sphere with the same diameter as the mesh aperture of the underlying sieve, or the weight of the sphere having the average diameter between the mesh apertures of adjacent sieves does not change the distribution of the resulting equivalent particle numbers. Materials in the largest and smallest sieves were excluded from the procedure because of their intrinsic sampling and sieving limits, respectively. Six particle classes were obtained, named equivalent particle size classes: 4 mm, 2 mm, 1 mm, 0.5 mm, 0.25 mm, and 0.125 mm.

Particle size analysis was performed by plotting equivalent particle numbers versus the corresponding equivalent size classes in bilogarithmic graphs and obtaining the corresponding fractal dimensions from the slope of the best fit lines. A sensitivity test was made by dividing three samples into two equivalent parts and analysing each of the two parts separately. Differences in the D values obtained from each sample (ΔD) are very small and start from the third decimal digit (Table 2 in the **Background Data Set**[1]). The use of samples collected in the same lithology allowed ruling out the influence of the rock type on D values.

2.2. Particle size distribution

Equivalent particle abundances in each size class align very well in bilogarithmic graphs (Fig. 4) and this supports the power-law distributions of particle sizes in the 4 mm–0.125 mm size range. As a general feature, the contribution of larger equivalent particles (4 mm, 2 mm, 1 mm equivalent size classes) to the total equivalent particle abundances is negligible. Samples with the lower D values pertain to the boundary regions of both strike-slip and extensional fault cores (Table 3 in the **Background Data Set**[1]). Fractal dimensions obtained from the breccia zones vary

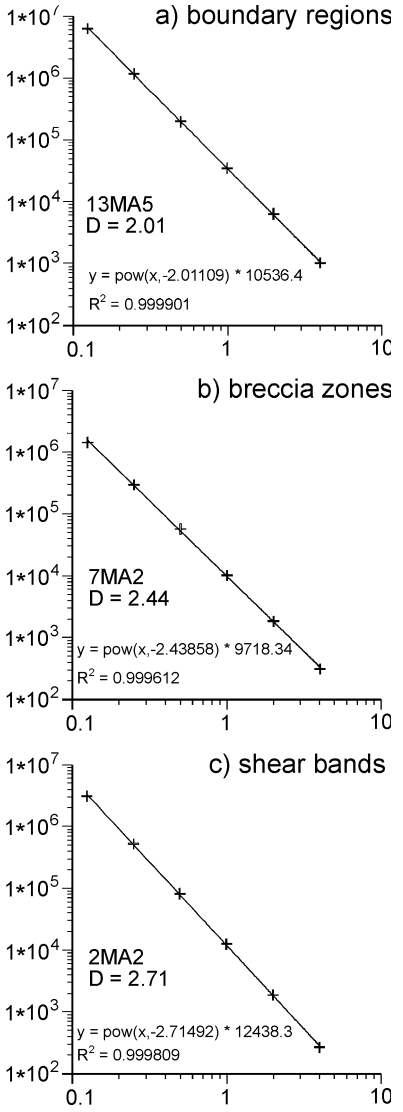

Fig. 4. Examples of linear fitting of particle size data in bilogarithmic graphs. (a) Sample 13MA5, collected in the boundary region of the cataclastic fault core. (b) Sample 7MA2, collected in the breccia zone. (c) Sample 2MA2, collected in a shear band.

from 2.17 to 2.74 in strike-slip fault cores and from 2.43 to 2.74 in extensional fault cores (Table 4 in the **Background Data Set**[1]). Fractal dimensions obtained from gouge in shear bands vary

←

Fig. 3. Typical fabrics of the main sectors within fault cores: (a) fault core boundary zone; (b) breccia zone; (c) gouge in a shear band within the breccia zone (approximately running from the lower left corner to the upper right corner).

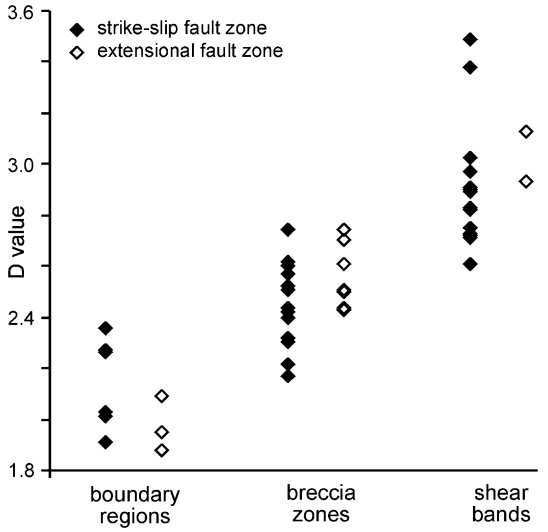

Fig. 5. Cumulative plot of the fractal dimensions D as a function of their position within the cataclastic fault cores and of fault kinematics.

from 2.61 to 3.49 in strike-slip fault cores (Table 5 in the **Background Data Set**[1]). Two gouge samples collected in extensional fault cores gave D values of 3.13 and 2.93 respectively. The summary plot of all data shows the variability of D with fault kinematics and the position within the fault core (Fig. 5). The complete overlap between D values obtained from both strike-slip and extensional fault cores does not support any significant influence of fault kinematics on the fractal dimension. On the other hand, there is a direct relation between the position of samples within fault cores and their D values. D values increase from the boundary regions to the shear bands. Partial overlap between different D populations indicates a gradual transition from differently evolved cataclastic fabrics.

3. Volumetric analysis

Volumetric data provide complementary information for a complete sample description. The distribution of cumulative volumes is shown in Fig. 6 for a representative set of samples selected according to the criterion of progressive increase of D values from 1.91 to 3.49. Volumes of equivalent particles were computed for samples normalised to a 1 kg standard weight. The volumetric fabric of cataclastic rocks constituting the boundary regions and breccia zones is dictated by larger particles, despite their negligible contribution to the total particle number. Conversely, in fault gouges the cumulative volume of small particles increases and eventually controls the rock fabric. This is illustrated by the progressive 'clockwise rotation' of the volumetric curves with increasing D. The shape of the volumetric curves evolves from near linear in sample 3MA1, curvilinear with an increasing downward convexity (samples 12MA2, 8MA3, 4MA1, 8MA2), to upward convex in sample RIO3 (Fig. 6). These shape changes are dictated by different behaviours of equivalent size classes with increasing D values. In particular, the cumulative volume of larger equivalent particles systematically decreases, whereas it systematically increases for smaller particles.

4. Particle population progression

Availability of samples from different structural positions within a single fault core allows inferring the evolution of particle size distributions

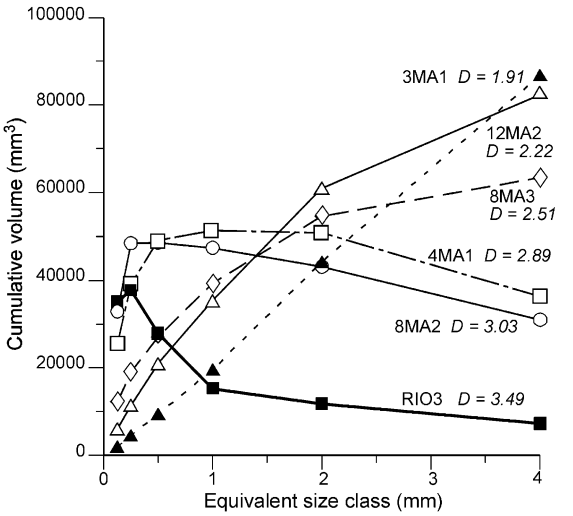

Fig. 6. Cumulative volume of equivalent particles plotted versus the corresponding equivalent size classes. Samples have been selected according to the criterion of progressive increase of D values from 1.91 to 3.49.

during the overall size reduction process from coarse-grained boundary zones, to breccia zones, up to the formation of gouge bands. Variations of normalised equivalent particle numbers with progressive cataclasis were analysed in sample pairs collected in the same fault cores (Fig. 2). Equivalent particle numbers in each size class of the higher-D sample were divided by the equivalent particle numbers in the corresponding size class of the lower-D sample. This on the basis of the assumption that D represents an effective parameter for describing the degree of comminution of cataclastic rocks and that higher-D cataclastic fabrics evolved from the lower-D ones [21]. Data normalisation implies the relative dependence of equivalent particle numbers in the various size classes. As a consequence, any increase of the equivalent particle number in the smaller size classes will induce a slight decrease in the larger ones.

In the following, we illustrate particle size progression for sample pairs selected as representative of the whole data set. A sample pair is compared for fault core 6MA, which basically consists of immature cataclastic rocks with a central band of more comminuted material, represented by sample 6MA2. Analysis of the ratio between corresponding equivalent particle numbers (Fig. 7a) points out a decrease of the larger equivalent particles, highlighted by a quotient lower than 1, and an increase of all other equivalent particles. In particular, the 0.25 mm equivalent size class almost doubles and the smaller equivalent particles (0.125 mm) are close to triplicate. The pair 7MA consists of a sample from the breccia zone (7MA2) and the other from a shear band (7MA1). Equivalent particle ratios (Fig. 7b) show a small relative variation of the 4 mm equivalent size class, which decreases by about 15%. All the other equivalent size classes are characterised by relative increments of the corresponding particle numbers, which generally increase with a decrease of the equivalent particle size. Only in the smaller equivalent size class is this increment lower than the corresponding one in the adjacent class. Fault core 8MA allows inferring the evolution of equivalent particle numbers within the breccia zone (samples 8MA1, 8MA3 and 8MA4) and the transition to fault gouge (sample 8MA2). The progression of the cataclastic fabric in the breccia zone from $D=2.4$ to $D\approx 2.5$ occurs through a generalised increase of equivalent particles apart from the larger ones, which remain almost unchanged (Fig. 7c). This increase becomes more pronounced with the decrease of the equivalent particle size. With increasing D values in the breccia zone rocks (samples 8MA3 and 8MA4), but maintaining the same ΔD (~ 0.1), the trend of the corresponding curve is very similar to the previous one but shifted downward by about 0.5 (Fig. 7c). When ΔD is doubled to about 0.2 (8MA4/8MA1) the upward convexity of the corresponding curve increases due to the preferential increase of intermediate and smaller equivalent particles. This behaviour is much more evident in the breccia to gouge transition (8MA4 to 8MA2), which occurs by a significant decrement of larger equivalent particles, by a small decrement of particles in the 2 mm equivalent size class, and by a large increment in the medium and small equivalent size classes. The increase of the smaller equivalent particle number is almost three times greater than the decrease of the larger equivalent particle number. The preferential increase of the smaller equivalent particles with increasing comminution (i.e. D) is confirmed by the behaviour of the weight of material passing through the smallest sieve (0.063 mm). Plotting this weight as a percentage of the total weight against the corresponding D value shows an exponentially increasing trend with increasing D (Fig. 8).

Fault core 11MA consists of a sample collected in the breccia zone (11MA2) and another in a shear band (11MA1). Analysis of the equivalent size class ratios (Fig. 7d) points out a small decrement of the 4 mm equivalent particles, characterised by a quotient lower than 1, while all the other equivalent size classes undergo significant increments, particularly the two smaller equivalent particle size classes. The increment of the smaller particles, which approaches 400%, is much greater than the decrement of the larger particles. Fault core 13MA is representative of the evolution of an immature cataclastic core. Sample 13MA5 was collected in the boundary re-

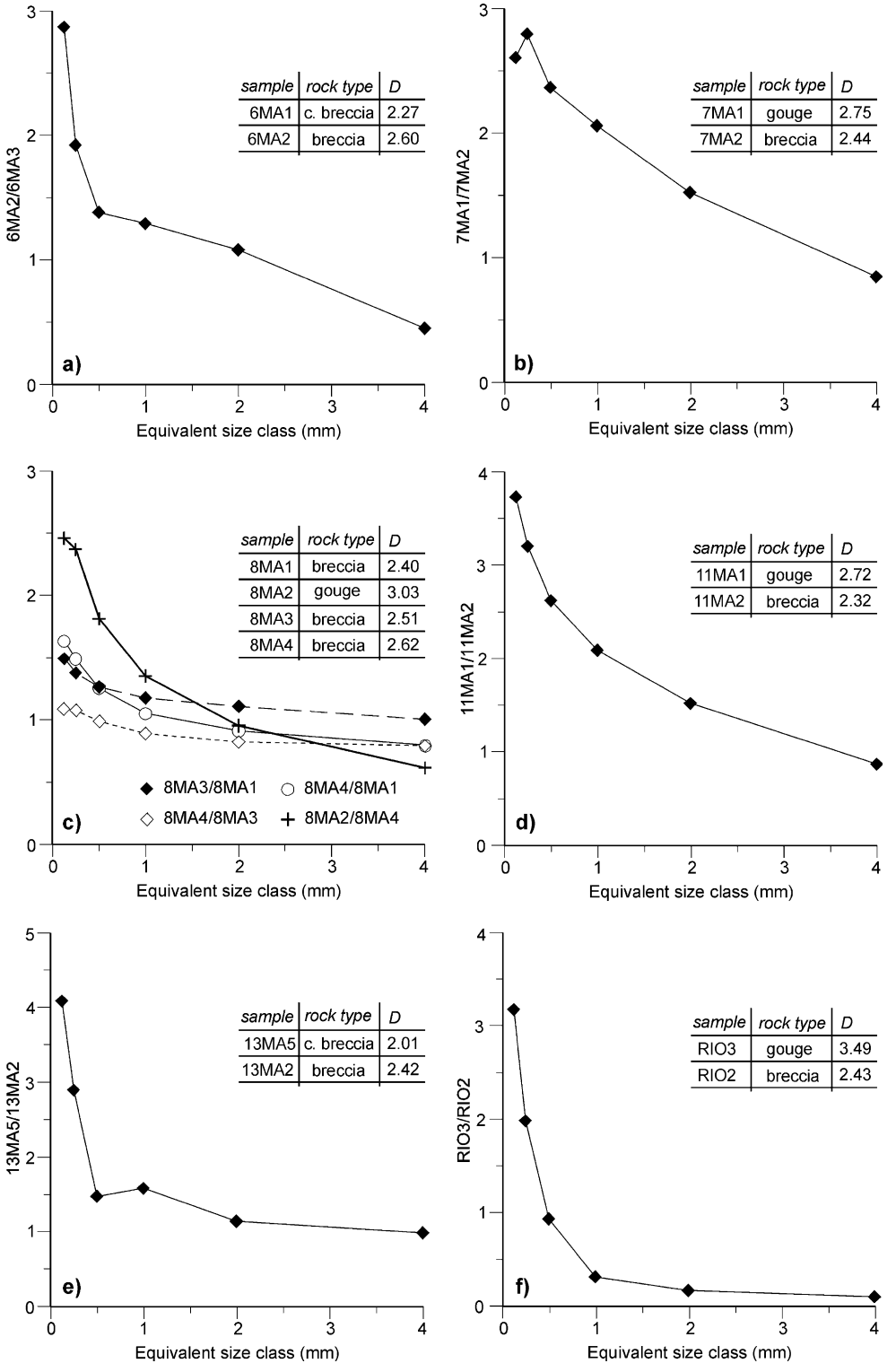
6MA2/6MA3
Equivalent size class (mm)
a)
sample | rock type | D
6MA1 | c. breccia | 2.27
6MA2 | breccia | 2.60
7MA1/7MA2
b)
sample | rock type | D
7MA1 | gouge | 2.75
7MA2 | breccia | 2.44
8MA3/8MA1
8MA4/8MA1
8MA4/8MA3
8MA2/8MA4
c)
sample | rock type | D
8MA1 | breccia | 2.40
8MA2 | gouge | 3.03
8MA3 | breccia | 2.51
8MA4 | breccia | 2.62
11MA1/11MA2
d)
sample | rock type | D
11MA1 | gouge | 2.72
11MA2 | breccia | 2.32
13MA5/13MA2
e)
sample | rock type | D
13MA5 | c. breccia | 2.01
13MA2 | breccia | 2.42
RIO3/RIO2
f)
sample | rock type | D
RIO3 | gouge | 3.49
RIO2 | breccia | 2.43

gion of the fault core and sample 13MA2 comes from the breccia zone. Analysis of the equivalent size class ratios (Fig. 7e) shows a great increment characterising the small equivalent particles (more than 300% in the 0.125 mm equivalent size class and about 200% in the 0.25 mm equivalent size class) compared to the almost invariant behaviour of the larger ones. The two intermediate equivalent size classes show a comparable increment of about 50%. Fault core RIO was selected as representative of the development of an extremely comminuted gouge band (RIO3) within the breccia zone (RIO2). Differing from all the previous cases, even intermediate particles show negative quotients (Fig. 7f). Particularly, the 4 mm, 2 mm and 1 mm classes are characterised by very small values, meaning that they underwent a significant decrement. Only values in the two smallest equivalent particle size classes greatly increase.

5. Discussion

5.1. Fractal dimensions

The main point arising from the particle size data is that the fractal dimensions of the studied cataclastic rocks do not cluster around a specific value but are distributed over a wide interval from 1.88 to 3.49. It should be noted that D values greater than 3 are not possible in the absence of fractal limits, because this would mean that total particle volume should be greater than available, i.e. particle interpenetration. It follows that the distributions of equivalent particles with D greater than 3 should have upper and lower fractal limits, above and below which these particle size distributions are no longer fractal [17,38]. The linear fits of our data imply that measured size classes lie within the linear (fractal) segments of the bilogarithmic distributions and that the upper and lower fractal limits are external to the 0.125–4 mm size interval.

The occurrence of large variations of D values questions the idea that cataclasis can be conveniently described by the thoroughgoing persistence of a fragmentation mechanism described by a fractal dimension $D \approx 2.6$ [13]. Conversely, our data suggest a progressive change of the fragmentation mechanism with increased intensity of comminution. This is indicated by the increase of D values from immature core boundary rocks, to breccia zones, up to intensely comminuted gouge in shear bands. The evidence that 2.6–2.7 is the highest fractal dimension in cataclastic rocks from breccia zones may suggest the idea that it represents a threshold value associated with a particularly favourable fragmentation mechanism [13]. When cataclastic rocks in breccia zones develop a fabric corresponding to this threshold value, their further evolution may continue in a near steady-state way [27].

An alternative hypothesis is that the cataclastic fabric associated with fractal dimensions of about 2.6–2.7 may enhance slip localisation [39] and the consequent formation of narrow shear bands where most displacement is accommodated. Slip localisation, in turn, induces a negative velocity dependence and a lowering of friction in these shear zones [40], facilitating the persistence of their activity. A self-enhancing cataclastic process may thus be triggered in narrow shear bands of localised slip, where intensely comminuted gouge develops, likely preventing further reworking of the cataclastic fabric in the adjacent breccia zones.

Relative comparison among differently evolved cataclastic rocks in the same fault core shows that the development of D values higher than 2.6–2.7 occurs, at least in 'massive' carbonate rocks, by the preferential relative increase of smaller particles rather than by the selective decrease of larger particles, as proposed for crystalline basement

←

Fig. 7. Ratios between the equivalent particle numbers in corresponding size classes in sample pairs collected from the same fault cores. These graphs show the relative increase or decrease of equivalent particles in each size class during the progression of cataclasis. See text for a discussion of the effect of data normalisation. (a) Ratio between samples 6MA2 and 6MA3. (b) Ratio between samples 7MA1 and 7MA2. (c) Ratio between samples 8MA3 and 8MA1, 8MA4 and 8MA1, 8MA4 and 8MA3, 8MA2 and 8MA4 respectively. (d) Ratio between samples 11MA1 and 11MA2. (e) Ratio between samples 13MA5 and 13MA2. (f) Ratio between samples RIO3 and RIO2. C. breccia means coarse-grained breccia, sampled in fault core boundary regions.

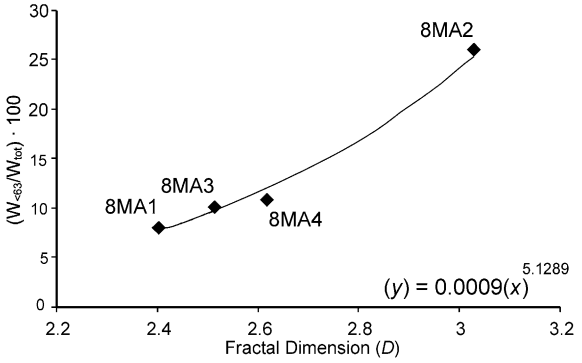

Fig. 8. Direct relationship between fractal dimensions and percentage weight of material having size smaller than 0.063 mm in the corresponding samples of fault core 8MA. The weight of the sample fraction with a particle size smaller than 0.063 mm was obtained by subtracting the residual dry weight after sieving to the total dry weight of the sample. Note that for $D \approx 3$ the weight of material with a particle size smaller than 0.063 mm is more than 26% of the sample total weight.

cataclastic rocks [14,27]. The increment of smaller equivalent particles is up to four times greater than the decrement of the larger equivalent particles (Figs. 7b–d,f and 8). A preferential increase of small particles with fault slip has been documented by [29] in large displacement laboratory experiments on quartz fault gouge.

The abundance of smaller particles in intensely comminuted cataclastic rocks cannot be explained by their preferential fragmentation because this contrasts with the notion of particle strength increase with decreasing size [41]. More likely, the increase of small particles in gouge bands is induced by slip-enhanced surface abrasion [37] during the progressive decrease of the average particle size, as pointed out by [26] in laboratory experiments, and by [21] in natural fault cores developed in granites. Survivor larger particles in intensely comminuted gouge are fully surrounded by small particles and this decreases their capability of being fractured [4,13,26,39]. The proposed evolutionary pathway for cataclastic rock fabrics in carbonate fault cores is schematically illustrated in Fig. 9. Early stages of fault core formation are dominated by particle fragmentation while particle abrasion controls the distribution of particle size and shape in fault gouge.

5.2. Influence on permeability properties

The broad variability of D values and the evidence of a preferential increase of smaller particles with increasing comminution have important consequences for the space and time evolution of fault permeability. The three-dimensional architecture of poorly evolved (i.e. low-D) cataclastic fabrics is dominated by the packing properties of larger particles and this favours a high porosity and an efficient permeability. An increase of D indicates an increased capability (i.e. greater number) of smaller particles to fill the available space between larger particles. The exponential direct relation between D and the amount of particles in the silt and clay size range (< 0.063 mm) obtained from fault core 8MA (Fig. 8) indicates that even very small voids are filled in fault gouges, which thus attain an extremely low permeability. This contributes to explain the hydraulic seal behaviour of gouge bands in natural fault zones [42,43] and in laboratory experiments [29]. The hydraulic seal behaviour of fault gouge developed in massive carbonate platform rocks can be inferred from some fault cores in the studied field sites. The boundary regions of these fault cores show strong impregnation by iron hydroxides, abruptly terminating at more comminuted breccia zone or gouge band

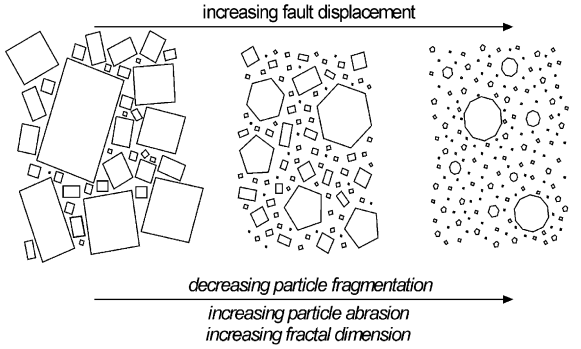

Fig. 9. Cartoon showing the proposed evolution of the cataclastic fabric with increasing displacement. The role of particle fragmentation in the comminution process progressively decreases and is replaced by particle abrasion. The increment of smaller particles produced by surface abrasion is much greater than the decrement of the larger particles, caused by their fragmentation.

Fig. 10. Detail of the abrupt transition from the fault core boundary zone to the breccia zone. The former is strongly impregnated by iron hydroxides (dark material on the left side of the photo). Whitish breccias are not impregnated attesting to their lower permeability. Note the dark stream of hydroxides at the boundary between the two sectors.

boundaries, which are characterised by the occurrence of almost continuous bands of iron hydroxides (Fig. 10). The lack of any evidence of hydroxide impregnation within the breccia zones or the gouge bands indicates that they acted as barriers to the across-fault migration of fluid phases. The lack of comminuted feldspars and phyllosilicates in these fault cores rules out the role of water-induced clay formation [11,43] on fault permeability properties. Conversely, the extremely low permeability of fault gouge in carbonate platform rocks is mainly related to the particle size distribution and packing.

Development of a fault zone is a four-dimensional process where different evolutionary stages occur in different structural positions. Faulting in limestone typically evolves from early joint and solution cleavage arrays (the damage zone), which are then overprinted by the formation of cataclastic rocks during slip localisation and the development of fault cores [44–46]. The progressive development of fault cores from damage zones implies that different permeability properties occur in different regions of fault zones at different evolutionary stages (Fig. 11). In the tip regions, fault zone growth is in an immature stage, where only the damage zone developed. The progression of fracturing in the damage zone increases permeability and connectivity and the whole fault zone behaves as a conduit for fluid flow. The lateral propagation of the low-permeability fault core dissects the across and along strike continuity of the conduit, causing its progressive compartmentalisation into sectors with low hydraulic exchanges. In this mature stage, the contrast between high-permeability damage zones and fault core boundary regions, and very low-permeability gouge bands within breccia zones imparts a directional anisotropy to permeability in fault zones, which act as conduits for fluid flow parallel to the fault strike and as barriers for fluid flow perpendicular to the fault strike [8,29].

5.3. Role of dissolution

Removal of material by dissolution, either syn- or post-tectonic, is a well-known phenomenon in carbonate rocks [47,48]. The efficiency of dissolution in limestone is maximised at low strain rates, high fluid flows, high ratios between surface and volume of particles, and when a certain amount of clay minerals occurs [49–51]. In the studied

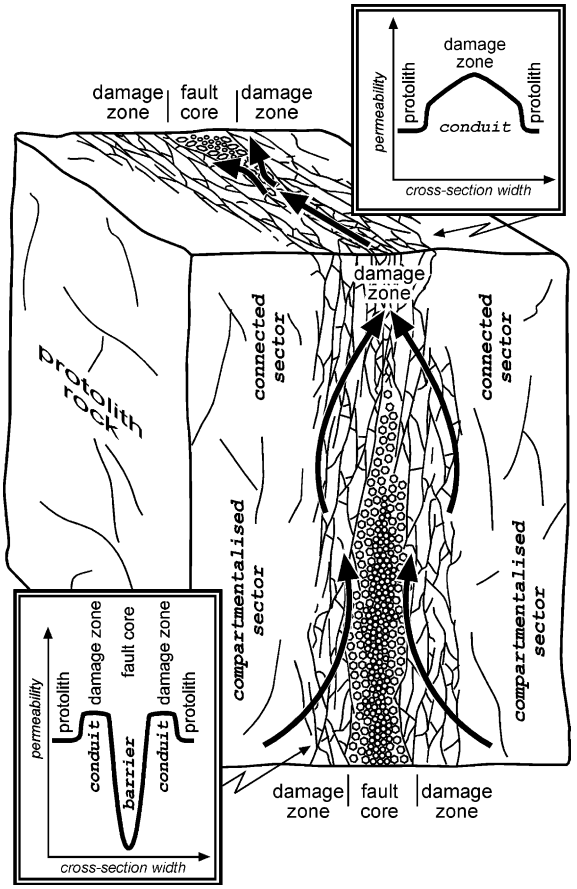

Fig. 11. Cartoon showing the permeability structure of an ideal fault zone in carbonate platform fault rocks. The tip line of the fault is imaged to propagate upward and from left to right. The two qualitative graphs schematically show the transition from a conduit to a barrier behaviour of the fault zone passing from an early (only damage zone) to a mature structural architecture. Arrows show the expected pathway of fluid phases within the fault zone. Not to scale.

fault zones, pressure solution cleavage arrays are well developed in damage zones [46], despite the very poor content of clayish material in the protolith rocks. This suggests low strain rates and efficient fluid circulation in the very early stages of faulting. Conversely, the preservation of the finest fraction in the sampled cataclastic rocks indicates a negligible role of dissolution during fault activity because smaller particles have the highest surface–volume ratio and thus should have been easily dissolved. Possible reasons for their preservation include high strain rates and/or inefficient fluid circulation. The latter is in agreement with the sub-aerial environmental conditions of deformation in the study faults, many of which are currently active [52,53].

Post-faulting fluid flow within the studied fault cores might have altered their original particle size distributions. The capability of meteoric water to dissolve carbonate fault rocks depends on D values. The increase of D from fault core boundaries to intensely comminuted gouge in shear bands implies a corresponding decrease of permeability and, consequently, of possible dissolution-related bias. The higher permeability of cataclastic rocks in the fault core boundary regions may have favoured the partial removal by dissolution of part of the smaller particles, producing a further decrease of D. Conversely, the lower permeability of cataclastic rocks in breccia zones may have inhibited a significant alteration of D values by dissolution. The same reasoning applies to fault gouge, whose very low permeability likely prevents any influence of dissolution, despite the extremely fine particle size.

6. Conclusions

We analysed particle size distributions in carbonate cataclastic rocks from fault cores in the Apennines, Italy. Particle sizes are power-law-distributed over the analysed size range and their fractal dimensions increase from the boundary zones of fault cores, to the breccia zones constituting the bulk of fault cores, up to intensely comminuted gouge in shear bands within breccia zones. Such a large variability of the fractal dimensions and its relationships with the structural architecture of fault cores indicate that the idea of a persistent fragmentation mechanism for describing the entire evolution of natural cataclastic fault cores in carbonate rocks is inadequate. We propose that the evolution of the cataclastic process in the studied fault cores involved: (i) a progressive change of the dominant fragmentation mechanism with increasing displacement; (ii) a relation between particle size distributions and fault slip; (iii) an increased contribution of surface abrasion with increasing displacement; (iv) the variation of

particle strength with size and shape. The non-self-similar evolution of cataclasis has important implications for the four-dimensional evolution of the permeability structure in carbonate fault cores and for their frictional behaviour.

Acknowledgements

This paper strongly benefited of critical reading and suggestions from EPSL reviewers M. Antonellini and T. Blenkinsop. This work has been funded by MURST grants awarded to F. Salvini, and by Enterprise Oil Italiana S.p.A. We are grateful to R. Gambini (formerly at Enterprise Oil Italiana S.p.A.) for encouraging our work and to P. Impagliazzo, S. Merlo and M. Musacchio for their help during field and laboratory work. A. Taddeucci and P. Tuccimei provided the chemical analyses of the protolith rocks. *[RV]*

References

[1] I. Borg, M. Friedman, J. Handin, D.V. Higgs, Experimental deformation of St. Peter sand: a study of cataclastic flow, Geol. Soc. Am. Mem. 79 (1960) 133–191.
[2] D.U. Wise, D.E. Dunn, J.T. Engelder, P.A. Geiser, R.D. Hatcher, S.A. Kish, A.L. Odom, S. Schamel, Fault-related rocks: Suggestions for terminology, Geology 12 (1984) 391–394.
[3] T. Shimamoto, J.M. Logan, Effects of simulated fault gouge on the sliding behavior of Tennessee sandstone: Nonclay gouges, J. Geophys. Res. 86 (1981) 2902–2914.
[4] C.A. Morrow, J.D. Byerlee, Experimental studies of compaction and dilatancy during frictional sliding on faults containing gouge, J. Struct. Geol. 7 (1989) 815–825.
[5] D.R. Scott, C.J. Marone, C.G. Sammis, The apparent friction of granular fault gouge in sheared layers, J. Geophys. Res. 99 (1994) 7231–7246.
[6] C. Marone, Laboratory-derived friction laws and their application to seismic faulting, Annu. Rev. Earth Planet. Sci. 26 (1998) 643–696.
[7] M. Antonellini, A. Aydin, Effect of faulting on fluid flow in porous sandstones: geometry and spatial distribution, Am. Assoc. Pet. Geol. Bull. 79 (1995) 642–671.
[8] J.S. Caine, J.P. Evans, C.B. Forster, Fault zone architecture and permeability structure, Geology 24 (1996) 1025–1028.
[9] J.T. Engelder, Cataclasis and the generation of fault gouge, Geol. Soc. Am. Bull. 85 (1974) 1515–1522.
[10] R.H. Sibson, Fault rock and fault mechanisms, J. Geol. Soc. London 133 (1977) 191–213.
[11] E.H. Rutter, R.H. Maddock, S.H. Hall, S.H. White, Comparative microstructures of natural and experimentally produced clay-bearing fault gouges, Pure Appl. Geophys. 124 (1986) 3–30.
[12] N. Yoshioka, Fracture energy and the variation of gouge and surface roughness during frictional sliding of rocks, J. Phys. Earth 34 (1986) 335–355.
[13] C. Sammis, G. King, R. Biegel, The kinematics of gouge deformation, Pure Appl. Geophys. 125 (1987) 777–812.
[14] T.G. Blenkinsop, Cataclasis and processes of particle size reduction, Pure Appl. Geophys. 136 (1991) 59–86.
[15] F.M. Chester, N.G. Higgs, Multimechanism friction constitutive model for ultrafine quartz gouge at hypocentral conditions, J. Geophys. Res. 97 (1992) 1859–1870.
[16] F.M. Chester, J.P. Evans, R.L. Biegel, Internal structure and weakening mechanisms of the San Andreas Fault, J. Geophys. Res. 98 (1993) 771–786.
[17] L.J. An, C.G. Sammis, Particle size distribution in cataclastic fault materials from Southern California: a 3-D study, Pure Appl. Geophys. 143 (1994) 203–228.
[18] J.P. Evans, F.M. Chester, Fluid-rock interaction in faults of the San Andreas system: Inferences from San Gabriel fault rock geochemistry and microstructures, J. Geophys. Res. 100 (1995) 13007–13020.
[19] J.K. Morgan, T.T. Cladouhos, K.M. Scharer, D.S. Cowan, P. Vrojlik, Fractal particle size distributions in Death Valley fault zones: Controls on mechanics and kinematics of fault rocks, Geol. Soc. Am. Abstract with Programs 29 (1997).
[20] T.T. Cladouhos, Shape preferred orientations of survivor grains in fault gouge, J. Struct. Geol. 21 (1999) 419–436.
[21] I. Hattori, H. Yamamoto, Rock fragmentation and particle size in crushed zones by faulting, J. Geol. 107 (1999) 209–222.
[22] J.D. Byerlee, V. Mjachkin, R. Summers, O. Voevoda, Structures developed in fault gouge during stable sliding and stick-slip, Tectonophysics 44 (1978) 161–171.
[23] Y. Gu, T.F. Wong, Development of shear localization in simulated fault gouge: Effects of cumulative slip and gouge particle size, Pure Appl. Geophys. 143 (1994) 387–423.
[24] C.G. Sammis, R.H. Osborne, J.L. Anderson, M. Banerdt, P. White, Self-similar cataclasis in the formation of fault gouge, Pure Appl. Geophys. 124 (1986) 54–77.
[25] W.L. Power, T.E. Tullis, J.D. Weeks, Roughness and wear during brittle faulting, J. Geophys. Res. 93 (1988) 15268–15278.
[26] R.L. Biegel, C.G. Sammis, J.H. Dieterich, The frictional properties of a simulated gouge having a fractal particle distribution, J. Struct. Geol. 11 (1989) 827–846.
[27] C.J. Marone, C.H. Scholz, Particle-size distribution and microstructures within simulated fault gouge, J. Struct. Geol. 11 (1989) 799–814.
[28] S.L. Karner, C. Marone, The effect of shear load on fric-

tional healing in simulated fault gouge, Geophys. Res. Lett. 25 (1998) 4561–4564.
[29] S. Zhang, T.E. Tullis, The effect of fault slip on permeability and permeability anisotropy in quartz gouge, Tectonophysics 295 (1998) 41–52.
[30] B. Bos, C.J. Peach, C.J. Spiers, Slip behavior of simulated gouge-bearing faults under conditions favoring pressure solution, J. Geophys. Res. 105 (2000) 16699–16717.
[31] K. Mair, I. Main, S. Elphick, Sequential growth of deformation bands in the laboratory, J. Struct. Geol. 22 (2000) 25–42.
[32] C.J. Allègre, J.L. Le Mouel, A. Provost, Scaling rules in rock fracture and possible implications for earthquake predictions, Nature 297 (1982) 47–49.
[33] D.L. Turcotte, Fractals and fragmentation, J. Geophys. Res. 91 (1986) 1921–1926.
[34] C.H. Scholz, Wear and gouge formation in brittle faulting, Geology 15 (1987) 493–495.
[35] K.J. Morgan, Numerical simulations of granular shear zones using the distinct element method. 2. Effects of particle size distribution and interparticle friction on mechanical behavior, J. Geophys. Res. 104 (1999) 2721–2732.
[36] C. Sammis, R.L. Biegel, Fractals, fault-gouge, and friction, Pure Appl. Geophys. 131 (1989) 256–271.
[37] R.LeB. Hooke, N.R. Iverson, Grain-size distribution in deforming subglacial tills role of grain fracture, Geology 23 (1995) 57–60.
[38] S.A. Steacy, C.G. Sammis, A damage mechanics model for fault zone friction, J. Geophys. Res. 97 (1992) 587–594.
[39] J.K. Morgan, M.S. Boettcher, Numerical simulations of granular shear zones using the distinct element method 1. Shear zone kinematics and the micromechanics of localization, J. Geophys. Res. 104 (1999) 2703–2719.
[40] N.M. Beeler, T.E. Tullis, M.L. Blampied, J.D. Weeks, Frictional behavior of large displacement experimental faults, J. Geophys. Res. 101 (1996) 8697–8715.
[41] N.J. Petch, The cleavage strength of polycrystals, J. Iron Steel Inst. 174 (1953) 25–28.
[42] J. Jackson, Living with earthquakes: know your faults, J. Earthq. Engin. 5 (2001) 5–123.
[43] C.A.J. Wibberley, T. Shimamoto, Internal structure and permeability of major strike-slip fault zones: the Median Tectonic Line in Mie Prefecture, Southwest Japan, J. Struct. Geol. 25 (2003) 59–78.
[44] E.J.M. Willemse, D.C.P. Peacock, A. Aydin, Nucleation and growth of strike-slip faults in limestones from Somerset, U.K., J. Struct. Geol. 19 (1997) 1461–1477.
[45] P.N. Mollema, M. Antonellini, Development of strike-slip faults in the dolomites of the Sella Group, Northern Italy, J. Struct. Geol. 21 (1999) 273–292.
[46] F. Salvini, A. Billi, D.U. Wise, Strike-slip fault-propagation cleavage in carbonate rocks: the Mattinata Fault zone, J. Struct. Geol. 21 (1999) 1731–1749.
[47] T.P. Engelder, A. Geiser, W. Alvarez, Role of pressure solution and dissolution in geology, Geology 9 (1981) 44–45.
[48] J. Hadizadeh, Interaction of cataclasis and pressure solution in a low-temperature carbonate shear zone, Pure Appl. Geophys. 143 (1994) 255–280.
[49] E.H. Rutter, The kinetics of rock deformation by pressure solution, Phil. Trans. R. Soc. London 283 (1976) 203–219.
[50] E. Rutter, Pressure solution in nature, theory and experiment, J. Geol. Soc. London 140 (1983) 725–740.
[51] J.-P. Gratier, F. Renard, P. Labaume, How pressure solution creep and fracturing processes interact in the upper crust to make it behave in both a brittle and viscous manner, J. Struct. Geol. 21 (1999) 1189–1197.
[52] P. Favali, R. Funiciello, G. Mattietti, G. Mele, F. Salvini, An active margin across the Adriatic Sea (central Mediterranean Sea), Tectonophysics 219 (1993) 109–117.
[53] N. D'Agostino, N. Chamot-Rooke, R. Funiciello, L. Jolivet, F. Speranza, The role of pre-existing thrust faults and topography on the styles of extension in the Gran Sasso range (central Italy), Tectonophysics 292 (1998) 229–254.